Available online at www.sciencedirect.com
SCIENCE DIRECT®
PERGAMON
Polyhedron 22 (2003) 1911–1916
POLYHEDRON
www.elsevier.com/locate/poly

A comparative high frequency EPR study of monomeric and dimeric Mn_4 single-molecule magnets

R.S. Edwards [a], S. Hill [a,*], S. Bhaduri [b], N. Aliaga-Alcalde [b], E. Bolin [a], S. Maccagnano [a], G. Christou [b], D.N. Hendrickson [c]

[a] Department of Physics, University of Florida, Gainesville, FL 32611, USA
[b] Department of Chemistry, University of Florida, Gainesville, FL 32611, USA
[c] Department of Chemistry and Biochemistry, University of California at San Diego, La Jolla, CA 92093, USA

Received 6 October 2002; accepted 10 January 2003

Abstract

We compare high frequency single crystal electron paramagnetic resonance (EPR) data for monomeric and dimeric Mn_4 complexes where, in the case of the latter, intra-dimer exchange interactions are known to significantly alter the low temperature quantum behavior. The monomeric system exhibits typical single-molecule $S = 9/2$ EPR spectra; analysis of these data have enabled us to characterize the effective spin Hamiltonian parameters for this material. In the dimeric system, the ground state transition shows a splitting over a narrow range of fields and frequencies. The transfer of spectral weight between these split peaks is consistent with the exchange bias picture which has been developed to explain the absence of a zero-field tunneling resonance in low temperature hysteresis experiments. Indeed, these measurements provide the first independent confirmation for this exchange bias model. The absence of a significant intensity in excited state EPR transitions for the dimer contrasts the results for the monomer. This likely suggests important differences concerning the coherence of excited states of the dimer versus the monomer. No clear indications for intermolecular exchange interactions were observed in the EPR for the monomer.

Keywords: Single-molecule magnets; Nanomagnet; Electron paramagnetic resonance; Quantum tunneling; Manganese

1. Introduction

Single-molecule magnets (SMMs) have attracted considerable recent interest [1–6]. Their main attraction is an intrinsic bistability which is realized via a large spin ground state (up to $26\mu_B$) and a significant axial (easy-axis) magnetocrystalline anisotropy [1]. This bistability has aroused great interest in terms of the use of SMMs in future molecular devices [2,6]. When grown as crystals, the magnetic unit is monodisperse—each molecule in the crystal has the same spin, orientation, magnetic anisotropy and structure. Thus, SMMs enable fundamental studies of properties intrinsic to magnetic nanostructures that have previously been inaccessible.

The property of magnetic bistability leads to hysteresis at low temperatures [7]. Unlike bulk magnets, this hysteresis is intrinsic to each individual molecule—hence the term SMM. However, essentially all SMMs continue to exhibit slow magnetic relaxation, even as $T \rightarrow 0$ K. This relaxation is caused by quantum tunneling, whereby interactions which break the axial symmetry of the molecule mix quantum states of opposite magnetic polarity [1,7]. One of the major goals in the design of future SMMs is to be able to control this quantum tunneling so that it may be exploited for possible applications. For example, tunneling should be suppressed if one is to use SMMs for data storage applications, whereas an ability to switch coherent tunneling on and off could prove useful for quantum computation [2].

In this article, we present high-frequency single crystal electron paramagnetic resonance (EPR) investigations for two SMM systems based on tetranuclear Mn

* Corresponding author. Tel.: +1-352-392-5711; fax: +1-352-392-3591.
E-mail address: hill@phys.ufl.edu (S. Hill).

0277-5387/03/$ - see front matter
doi:10.1016/S0277-5387(03)00239-0

complexes. In the first, the basic unit is monomeric, having the formula $[Mn_4O_3(OSiMe)_3(O_2CEt)_3(dbm)_3]$ (denoted SB4 for short). This complex has been shown to exhibit all of the typical properties of a SMM, including low temperature hysteresis loops that exhibit quantum steps due to resonant magnetic quantum tunneling (MQT) [8,9]. In the second complex, the magnetic unit consists of a dimer of Mn_4 cubes, with the formula $[Mn_4O_3Cl_4(O_2CEt)_3py_3]_2$ (denoted NA3 for short) [10]. Hysteresis experiments for this complex also show resonant MQT steps [6]. However, no tunneling is seen in zero-field—a behavior which is quite different from that observed for the monomeric system (SB4 [8,9]). Furthermore, the first tunneling transition is observed before one reaches zero-field on the down-sweeps of the hysteresis loops. Wernsdorfer et al. attribute these observations to antiferromagnetic intra-dimer magnetic interactions [6]; the magnitude of the effect suggests weak superexchange interactions via the Cl···Cl and C–H···Cl contacts between the two molecules within the dimer. This superexchange results in an antiferromagnetic exchange bias, whereby each half of the dimer acts as a field bias on its neighbor, resulting in a complete suppression of the zero-applied-field quantum tunneling resonance.

While the evidence for antiferromagnetic exchange within the dimer (NA3) is quite compelling, weaker anomalies are observed in the hysteresis loops for the SB4 monomer [8]. These anomalies, or fine structures, have also been explained as being caused by very weak many spin (exchange) interactions between near neighbor SMMs; in this case, the exchange pathway is believed to involve inter-molecular hydrogen bonding along chains of SMMs. In contrast to NA3, however, the effective coupling is ferromagnetic [8]. While the exchange description proposed by Wernsdorfer et al. successfully explains the observed hysteresis loops in SB4 and NA3, no independent confirmation has been published.

The Mn_4 unit for both SB4 and NA3 has a well isolated $S = 9/2$ ground state [6,8,9]. The effective spin Hamiltonian for an isolated SMM can be written [11]

$$\hat{H}_i = D\hat{S}_{zi}^2 + E(\hat{S}_{xi}^2 - \hat{S}_{yi}^2) + \mu_B \vec{B}\cdot\vec{g}\cdot\vec{S}_i + \hat{O}_4 + \hat{H}_i' \qquad (1)$$

where $\hat{S}_i$ is the single spin operator with components $\hat{S}_{xi}$, $\hat{S}_{yi}$, and $\hat{S}_{zi}$; D (<0) is the uniaxial anisotropy constant and E characterizes the transverse anisotropy in the plane perpendicular to the easy axis; g is the Landé g-factor and $\vec{B}$ is the applied magnetic field; $\hat{O}_4$ denotes weak fourth order crystal field terms; and $\hat{H}_i'$ describes additional perturbations that take into account disorder, and intermolecular dipolar and exchange interactions [12]. Ignoring transverse terms in Eq. (1), the energy spectrum consists of $(2S+1)$ levels which can be labeled according to the projection (M_{Si}) of the spin along the magnetic easy axis of the molecules. For a field applied parallel to the easy axis, this gives rise to $2S$ possible EPR transitions corresponding to $\Delta M_S = \pm 1$.

In the case of two coupled SMMs, as is the case for NA3, the effective two-spin Hamiltonian is written as a sum [6]

$$\hat{H} = \hat{H}_1 + \hat{H}_2 + J\hat{S}_1\cdot\hat{S}_2 \qquad (2)$$

where $\hat{H}_1$and $\hat{H}_2$ are given by Eq. (1); the cross term describes the superexchange coupling between the two molecules within the dimer, and J characterizes the strength of this coupling. This adds to the complexity of the energy level diagram, resulting in $(2S+1)\times(2S+1)$ levels. For NA3, the antiferromagnetic coupling (positive J) results in a zero-field ground state comprised of the degenerate (9/2, −9/2) and (−9/2, 9/2) levels, as shown in Fig. 1. However, application of a field ($\|z$) exceeding the exchange bias ($\sim$0.3 T) results in a crossing of the degenerate (−9/2, 9/2)/(9/2, −9/2) levels, and the (−9/2, −9/2) level, thereby changing the ground state to the latter (see Fig. 1).

In terms of the EPR, the exchange coupling results in two distinct single-spin transitions from each two-spin state, i.e. (M_{S1}, M_{S2}) to ($M_{S1}+1$, M_{S2}) or (M_{S1}, M_{S2}) to (M_{S1}, $M_{S2}+1$). However, more importantly, because of the exchange bias, the single-spin transitions now depend on the state of the other spin within the dimer. Thus, the first transitions from the two ground states, (9/2, −9/2) to (9/2, −7/2) and (−9/2, −9/2) to (−9/2, −7/2), have slightly different energies even though they both correspond to the same −9/2 to −7/2 single-spin transition. This situation is illustrated in Fig. 1. It is also now possible to excite multi-spin EPR transitions within this coupling scheme [8], though this should represent a much weaker (higher order) process. Single crystal EPR measurements enable us to test the above hypotheses, as

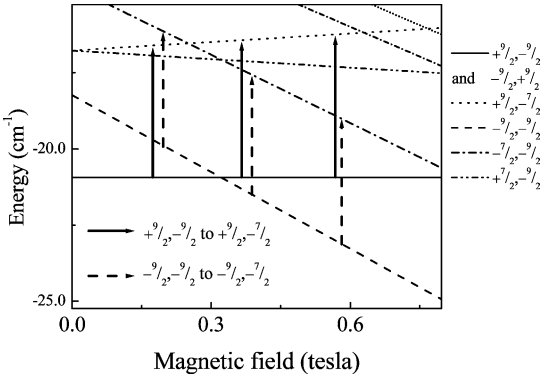

Fig. 1. The low lying two-spin energy levels for the NA3 dimer plotted as a function of magnetic field; the most important levels have been labeled according to the scheme described in the main text. For simplicity, the calculations of these levels ignored the transverse terms in Eqs. (1) and (2).

well as providing other important information such as the symmetries of the transverse crystal field terms that give rise to the observed tunneling [11].

2. Experimental

The $(2S+1)$-fold quantum energy level structure associated with a large molecular spin necessitates spectroscopies spanning a wide frequency range. Furthermore, large zero-field level splittings, due to the significant crystalline anisotropy (large D) and large total spin S, demand the use of frequencies and magnetic fields considerably higher (40 GHz to several 100 GHz, and up to 10 T respectively) than those typically used by the majority of EPR spectroscopists. Furthermore, in order to focus precisely on the exchange bias effect, it is essential to be able to tune the frequency fairly precisely over rather narrow frequency intervals. The latter requirement seemingly conflicts with the fact that one should use a narrow-band cavity perturbation technique in order to achieve the high-sensitivities necessary for single crystal work. To get around this problem, we use oversized cylindrical cavities, with fundamental modes well below 100 GHz. The tunability of our spectrometer (Millimeter-wave Vector Network Analyzer—MVNA) then enables us to tune to a multitude of fairly closely spaced higher order modes of the cavity; further technical details of this instrumentation are published elsewhere [13]. By placing the sample on one of the surfaces of the cavity, the boundary conditions for electromagnetic waves assure us that the a.c. and d.c. magnetic field polarizations are correct for observing EPR. Q-values well in excess of 10^3 are still obtained for many of these higher order modes. Typically, one finds several good modes over a 10 GHz interval, as well as many weaker modes which are often sufficient for following strong EPR transitions. For the studies on NA3 described below, we were able to follow the ground state transition at roughly 2 GHz intervals in the frequency range from about 130 to 145 GHz. Despite working on high order modes, the cavity technique still eliminates essentially all of the problems associated with standing waves that plague single-pass techniques [11]. Thus, the obtained resonances are symmetric, and they enable extremely detailed studies of the evolution of EPR line shapes as a function of frequency, temperature, magnetic field and field orientation.

The high symmetry SB4 crystals were needle like, with approximate dimensions $1.4 \times 0.16 \times 0.16$ mm^3. Very precise alignment ($< 0.2^\circ$) of the field was achieved via in situ rotation in a plane containing the needle axis. The easy axis for the smaller NA3 sample (dimensions $0.4 \times 0.3 \times 0.2$ mm^3) was not so easy to locate, and required several attempts, including in situ rotation about several axes. Data presented in this paper correspond to field alignment with the easy axis to no better than about 15–20°. Nevertheless, this is sufficient for achieving the main goals of this preliminary investigation. Details concerning the preparation of NA3 are given in ref. [10]. Temperature control between 2 and 300 K was achieved using a variable flow cryostat, and magnetic fields of up to 6 T were available from a split-coil superconducting magnet [13].

3. Results and discussion

3.1. The Mn_4 monomer

Fig. 2 shows the cavity transmission for a set of field sweeps taken for SB4 with the applied field aligned with the easy axis; the frequency is 138 GHz and the temperatures are indicated in the figure. Within this field range, five of the nine expected EPR transitions can clearly be seen as dips (absorptions) in the cavity transmission. The spacing between the resonances is more-or-less equal; a slight decrease in the spacing at higher fields is caused by a quartic crystal field term $\hat{O}_4^0$ in $\hat{H}_i'$ (see Eq. (1) and Fig. 3). Upon cooling, all of the intensity goes into the lowest field resonance, which corresponds to the $M_S = -9/2$ to $-7/2$ transition from the ground state to the first excited state. This, and the frequency dependence of the easy axis transitions (Fig. 3), confirm the total spin $S = 9/2$ of the molecule and the negative sign of D. The fit to the easy axis resonance positions (Fig. 3) is insensitive to the transverse terms in Eq. (1), to within sensible ranges of the coefficients. Therefore, it provides an excellent constraint on the diagonal terms (D, B_4^0, and $g_\parallel$) which we then use as a

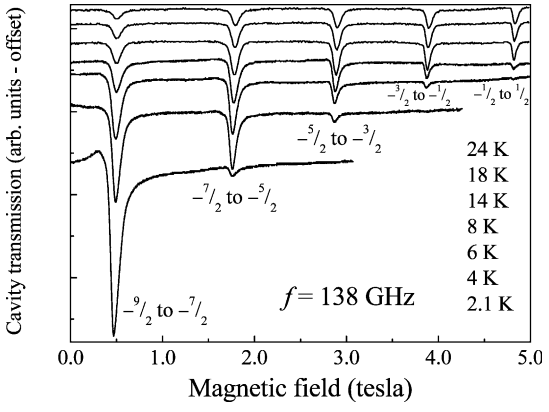

Fig. 2. Temperature dependence of a representative set of easy axis spectra (field$\|z$) for SB4. The temperatures and the frequency are indicated in the figure. The cavity transmission minima correspond to EPR transitions, which have been labeled accordingly; the traces are offset for clarity.

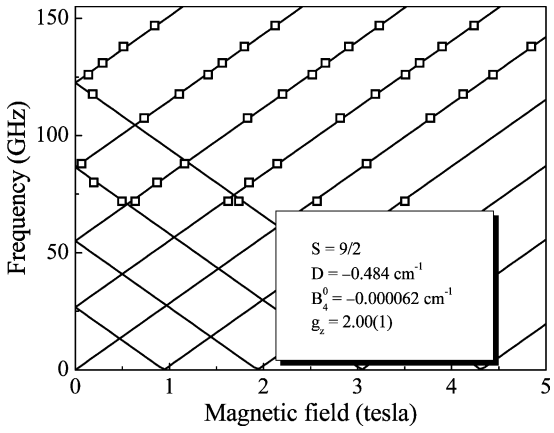

Fig. 3. Fits to the easy axis data for SB4, according to Eq. (1). The solid data points correspond to the resonance field positions obtained from measurements at several different frequencies; the solid lines represent the best fit. All data were taken at a temperature of 10 K. The obtained diagonal spin Hamiltonian parameters are listed in the inset.

basis for determining B_4^4 and $g_\perp$ from the transverse spectra; the obtained parameters are indicated in Fig. 3.

The measurements were repeated with the field applied within the hard plane of the sample, as shown in Fig. 4. For this orientation, all nine ($=2S$) resonances are observed, and the intensity of the transitions is reversed in comparison to the easy axis spectra, i.e. the transition from the ground state to the first excited state is observed at the highest field. A few weak low-field resonances are due to double quantum transitions, which are allowed for this orientation due to the strong mixing of levels in the transverse applied field. An exceptional fit to the frequency dependence of the hard axis data is obtained without including any additional parameters to those deduced from the easy axis spectra, as shown by the thick solid lines in Fig. 5. This is consistent with the high symmetry (C_3) of the SB4 molecule. For comparison, the fainter lines in Fig. 5

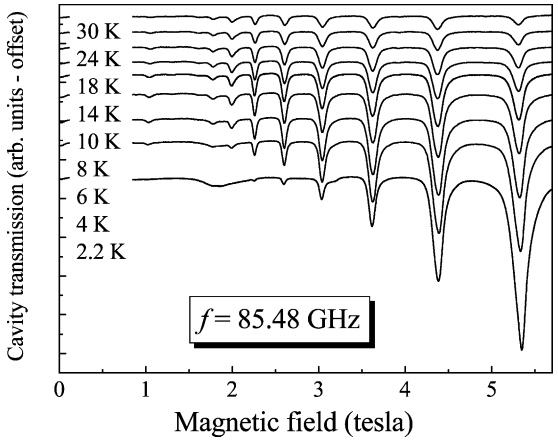

Fig. 4. Hard axis spectra for SB4. The temperatures and the frequency are indicated in the figure; the traces are offset for clarity.

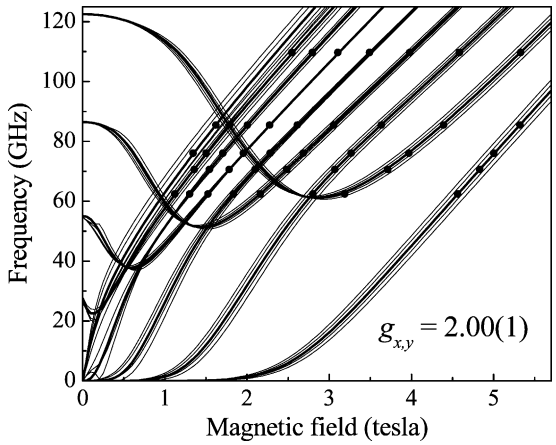

Fig. 5. Fits to the hard axis data for SB4, according to Eq. (1). All data were taken at a temperature of 10 K. The solid data points correspond to the resonance field positions obtained from measurements at several different frequencies. The thick solid line represents the best fit, using the same parameters as those listed in Fig. 3. The thin lines represent simulations which include a small quadratic anisotropy; the details of these simulations are discussed in the main text.

were generated by including a quadratic transverse anisotropy with a coefficient $E = 0.02$ cm^{-1}. In spite of the C_3 symmetry of the molecule, solvent disorder can give rise to local rhombic distortions [14,15]. Indeed, neutron scattering [16] and magnetic relaxation [9] experiments indicate appreciable transverse interactions, suggesting an E value of this order. Since the nature of the solvent disorder is not exactly known, nor is the precise field alignment within the hard (x, y) plane in our experiment, the thin lines in Fig. 5 were generated for field alignments of 0, 30, 60 and 90° relative to the x-axis. Because of the C_3 symmetry, solvent disorder should produce fine structure with a spread given by the faint lines in Fig. 5, similar to what has been seen in Mn_{12}–Ac [14,15]. To within the accuracy of the data, we cannot detect any evidence for such a quadratic transverse anisotropy. Indeed, derivatives of the hard axis spectra show no fine structure at all. Furthermore, the EPR linewidths are considerably less than the predicted spread. Therefore, it seems likely that the transverse interactions which have been detected for SB4 are due to higher order crystal field terms. In fact, higher order terms of magnitude necessary to account for the measured tunnel splittings [9,16] produce undetectable changes to the optimum fits in Figs. 3 and 5 (thick solid line).

Little or no indications for exchange bias were obtained from these experiments on SB4, although an unusual asymmetry in the lowest temperature data in Fig. 2 is not presently understood. Instrumental effects can be ruled out [13]. Therefore, the unusual lineshape seems to be real, and future investigations will focus on this aspect of the data.

3.2. The Mn_4 dimer

The easy axis spectra obtained for NA3 (Fig. 6) show some similarities to the easy axis data obtained for SB4 (Fig. 2). The strongest peak in Fig. 6 corresponds to excitations from the ground state of the dimer which, at this high frequency (185.2 GHz) and field, corresponds to the (−9/2, −9/2) state (see Fig. 1). Based on the simple exchange bias scheme developed by Wernsdorfer et al. [6], we can also assign labels to the higher field resonances in Fig. 6, and make a rough estimate of the axial crystal field parameters $D \approx -0.500\ \mathrm{cm}^{-1}$ and $B_4^0 \approx -7 \times 10-^5\ \mathrm{cm}^{-1}$; details of this analysis will be published elsewhere [17].

As expected for a transition from the ground state, the intensity from all excited level transitions (higher field resonances) goes into the ground state transition as T → 0. In principle, there are two possible excitations from the ground state, corresponding to (−9/2, −9/2) to (−9/2, −7/2) and (−9/2, −9/2) to (−7/2, −9/2) and, according to Eq. (2), one should expect a (tunnel) splitting of the symmetric and antisymmetric combinations of the (−9/2, −7/2) and (−7/2, −9/2) states. However, no clear evidence for this splitting was found from these EPR investigations. As the temperature is raised, it is noticeable that the ground state transition (strongest peak) loses intensity in a very similar fashion to the ground state transition for the monomer (Fig. 2). However, we see very little of this intensity showing up in the excited state transitions (compare Figs. 2 and 6). Part of the reason for this is due to the fact that there are now many more excited states of the dimer in close proximity to the first excited state (see Fig. 1). However, in the high field limit (B > exchange bias), the effect of the exchange bias on the transition frequencies (energy differences) is rather small [18], and one expects EPR spectra that are quite similar to the single-molecule case (SB4). Thus, it is surprising that we do not see intensity showing up as EPR transitions from excited levels, since the single-molecule crystal field parameters are rather similar for the monomer and the dimer. One possible explanation could be that most or all of the excited states of the dimer are very short lived, since the lifetime of each two-spin state now depends on the coherence of both molecules within the dimer.

The ability to measure at many different frequencies allows us to tune the ground state transition (main peak in Fig. 6) to the field region where the ground state level crossing occurs in Fig. 1. In this field range, a pronounced splitting becomes apparent in the lowest field resonance, as shown in Fig. 7, i.e. the exchange bias has a significant affect on the EPR in this low field limit. The data in Fig. 7 were obtained at 2 K, so as to enhance the intensity of the ground state transition(s). For clarity, the 3D plot in Fig. 7 was made with Lorentzian fits to the data, rather than the raw data, because the signal-to-noise ratio varies considerably for the different frequencies employed. It is a unique experimental achievement to be able to make narrow band cavity measurements on such a small single crystal, and at 2 GHz intervals above 130 GHz. The splitting is due to the different energies of the respective (9/2, −9/2) to (9/2, −7/2) and (−9/2, −9/2) to (−9/2, −7/2) ground state transitions (see Fig. 1). This splitting is very robust, and is simply due to the exchange bias, i.e. this has nothing to do with symmetric and antisymmetric

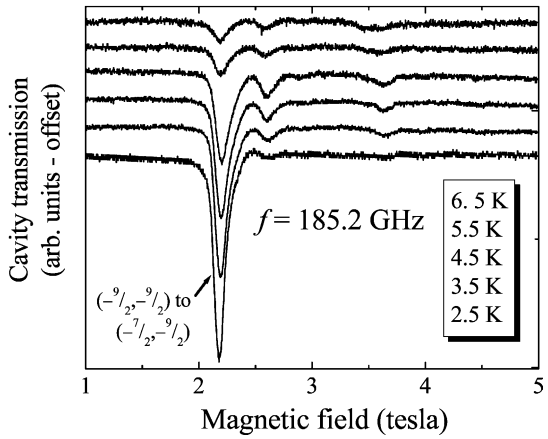

Fig. 6. Temperature dependence of a representative set of easy axis spectra (field approximately parallel to z) for NA3. The temperatures and the frequency are indicated in the figure. The cavity transmission minima correspond to EPR transitions. The strongest peak corresponds to transitions from the ground state of the dimer, and has been labeled according to the scheme described in the main text; the traces are offset for clarity.

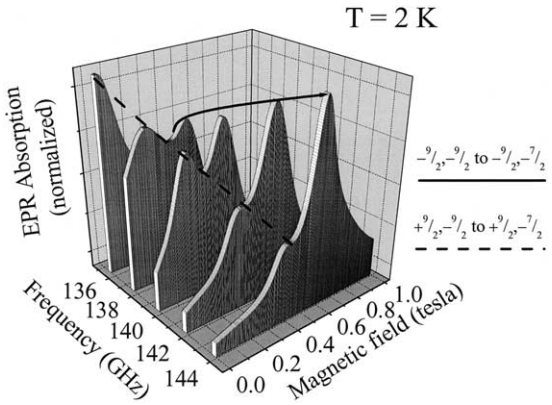

Fig. 7. A 3D plot of Lorentzian fits to the ground state transition(s) in NA3 obtained over a narrow field and frequency range; for clarity, the data correspond to Lorentzian fits to the original raw data. A pronounced splitting is apparent, which is due to the different frequencies of the respective (9/2, −9/2) to (9/2, −7/2) and (−9/2, −9/2) to (−9/2, −7/2) ground state transitions. By following the exchange-bias split resonances through the exchange bias field region (∼0.3 T), it is apparent that the intensity smoothly transfers from the (9/2, −9/2) to (9/2, −7/2) transition to the (−9/2, −9/2) to (−9/2, −7/2) transition. This observation is consistent with the change in the ground state of the dimer at ∼0.3 T.

combinations of excited states that were discussed above. By following the exchange-bias split resonance through the exchange bias field region (~ 0.3 T), it is apparent that the intensity transfers smoothly from the (9/2, −9/2) to (9/2, −7/2) transition to the (−9/2, −9/2) to (−9/2, −7/2) transition. This observation is consistent with the change in the ground state of the dimer at ~ 0.3 T. Furthermore, the switch in intensity occurs in the correct sense according to Eqs. (1) and (2), i.e. the high field peak grows with increasing field, and vice versa. The intensities become roughly equal when the split resonance is centered about 0.3 T, in agreement with the exchange bias field determined by Wernsdorfer et al. [6]. Therefore, these data provide substantial support for the exchange bias model.

Using a simple model which neglects transverse terms in Eq. (2), we can predict the expected splitting of the (9/2, −9/2) to (9/2, −7/2) and (−9/2, −9/2) to (−9/2, −7/2) ground state transitions. Surprisingly, the splitting should be twice the exchange bias field, yet we observe a substantially reduced value of about 0.2 T. However, this difference does not in any way invalidate the exchange bias model, which is based on the properties of the ground state. It merely tells us that we need to develop a more complete picture of the EPR, which involves excited levels as well; this is a work in progress [17].

4. Summary and conclusions

We compare single crystal EPR spectra for two tetranuclear Mn complexes, one monomeric and one dimeric. In the dimeric system (NA3), the ground state transition shows a splitting over a narrow range of fields and frequencies. The transfer of spectral weight between these split peaks is consistent with the exchange bias picture which has been developed to explain the absence of a zero-field tunneling resonance in low temperature hysteresis experiments [6]. Indeed, these measurements provide the first independent confirmation for this exchange bias model. The absence of a significant intensity of excited state EPR transitions for the dimer contrasts the results for the monomer. This likely suggests important differences concerning the coherence of excited states of the dimer versus the monomer. The monomeric system (SB4) exhibits typical single-molecule $S = 9/2$ EPR spectra, with no indications for intermolecular exchange interactions.

Acknowledgements

We thank Naresh Dalal, Andrew Kent and Wolfgang Wernsdorfer for stimulating discussion. Funding is provided by the National Science Foundation (DMR 0103290 and DMR 0196430) and by Research Corporation.

References

[1] G. Christou, D. Gatteschi, D.N. Hendrickson, R. Sessoli, MRS Bull. 25 (2000) 66.
[2] M.N. Leuenberger, D. Loss, Nature 410 (2001) 789.
[3] A. Mukhin, B. Gorshunov, M. Dressel, C. Sangregorio, D. Gatteschi, Phys. Rev. B 63 (2001) 214411.
[4] S. Parsons, C. Paulsen, F. Semadini, V. Villar, W. Wernsdorfer, R.E.P. Winpenny, Chem. Eur. J. 8 (2002) 4867.
[5] J.J. Sokol, A.G. Hee, J.R. Long, J. Am. Chem. Soc. 124 (2002) 7656.
[6] W. Wernsdorfer, N. Aliaga-Alcalde, D.N. Hendrickson, G. Christou, Nature 416 (2002) 406.
[7] E.M. Chudnovsky, J. Tejada, Macroscopic Quantum Tunneling of the Magnetic Moment, Cambridge University Press, Cambridge, 1998.
[8] W. Wernsdorfer, S. Bhaduri, R. Tiron, D.N. Hendrickson, G. Christou, Phys. Rev. Lett. 89 (2002) 197201.
[9] W. Wernsdorfer, S. Bhaduri, C. Boskovic, G. Christou, D.N. Hendrickson, Phys. Rev. B 65 (2002) 180403(R).
[10] D.N. Hendrickson, G. Christou, E.A. Schmitt, E. Libby, J.S. Bashkin, S. Wang, H.-L. Tsai, J.B. Vincent, P.D.W. Boyd, J.C. Huffman, K. Folting, Q. Li, W.E. Streib, J. Am. Chem. Soc. 114 (1992) 2455.
[11] S. Hill, S. Maccagnano, K. Park, R.M. Achey, J.M. North, N.S. Dalal, Phys. Rev. B 65 (2002) 224410.
[12] K. Park, M.A. Novotny, N.S. Dalal, S. Hill, P.A. Rikvold, Phys. Rev. B 66 (2002) 144409.
[13] M. Mola, S. Hill, M. Gross, P. Goy, Rev. Sci. Instrum. 71 (2000) 186.
[14] S. Hill, R.S. Edwards, J.M. North, K. Park, N.S. Dalal, arXiv: cond-mat/0301599 (2003); Phys. Rev. Lett. (2003), accepted for publication.
[15] A. Cornia, R. Sessoli, L. Sorace, D. Gatteschi, A.L. Barra, C. Daiguebonne, Phys. Rev. Lett. 89 (2002) 257201.
[16] A. Sieber, S. Bhaduri, H. Güdel, G. Christou, D.N. Hendrickson (unpublished).
[17] R.S. Edwards, S. Hill, S. Bhaduri, N. Aliaga, E. Bolin, S. Maccagnano, G. Christou, D.N. Hendrickson, in preparation.
[18] The exchange term in Eq. (2) only causes significant splittings of single-spin transitions in cases where one of the spin states in the dimer is completely reversed, e.g. (−9/2, 9/2) to (−7/2, 9/2) and (−9/2, −9/2) to (−7/2, −9/2).